J|A|C|S
ARTICLES
Published on Web 01/25/2003

Controlled Assembly of Carbon Nanotubes by Designed Amphiphilic Peptide Helices

Gregg R. Dieckmann,*,† Alan B. Dalton,‡ Paul A. Johnson,§ Joselito Razal,†,‡ Jian Chen,|| Geoff M. Giordano,† Edgar Muñoz,‡ Inga H. Musselman,† Ray H. Baughman,†,‡ and Rockford K. Draper§

Contribution from the Department of Chemistry, The University of Texas at Dallas, 2601 North Floyd Road, Richardson, Texas 75083-0688, NanoTech Institute, The University of Texas at Dallas, 2601 North Floyd Road, Richardson, Texas 75083-0688, Department of Molecular and Cell Biology, The University of Texas at Dallas, 2601 North Floyd Road, Richardson, Texas 75083-0688, and Zyvex Corporation, 1321 North Plano Road, Richardson, Texas 75081-2426

Received October 24, 2002; E-mail: dieckgr@utdallas.edu.

Abstract: Carbon nanotubes have properties potentially useful in diverse electrical and mechanical nanoscale devices and for making strong, light materials. However, carbon nanotubes are difficult to solubilize and organize into architectures necessary for many applications. In the present paper, we describe an amphiphilic α-helical peptide specifically designed not only to coat and solubilize carbon nanotubes, but also to control the assembly of the peptide-coated nanotubes into macromolecular structures through peptide−peptide interactions between adjacent peptide-wrapped nanotubes. The data presented herein show that the peptide folds into an amphiphilic α-helix in the presence of carbon nanotubes and disperses them in aqueous solution by noncovalent interactions with the nanotube surface. Electron microscopy and polarized Raman studies reveal that the peptide-coated nanotubes assemble into fibers with the nanotubes aligned along the fiber axis. Most importantly, the size and morphology of the fibers can be controlled by manipulating solution conditions that affect peptide−peptide interactions.

Introduction

The miniaturization of electronic circuitry is required for faster and more advanced applications. As the lower size limit of silicon-based circuitry is approached, molecular electronics, based in part on carbon nanotubes, are being investigated as an alternative technology. Carbon single-walled nanotubes (SWNTs) are single sheets of graphite rolled into seamless cylinders with diameters ranging from ∼0.5 to 5 nm and lengths that can exceed 1 μm.[1] Carbon nanotubes are either conductors (metallic) or semiconductors, depending on their diameter and the spiral alignment of the hexagonal rings of graphite along the tube axis, and they have very high tensile strengths.[1] Although there is intense interest in exploiting the novel properties of carbon nanotubes in electrical and mechanical devices,[2−6] carbon nanotubes are extremely hydrophobic and form insoluble aggregates that are difficult to assemble into useful structures.

Biological systems have evolved complex architectures created through the self-assembly of biological macromolecules. Evolution has thus provided biological molecules with a wide variety of intricate structures tailored for controlled self-assembly that might be adapted to the nanoscale self-assembly of nonbiological materials, such as carbon nanotubes. One structural motif used by proteins to promote self-assembly is the amphiphilic α-helix.[7] An α-helix is a protein secondary structure in which the polypeptide backbone forms a folded spring-like conformation stabilized by hydrogen bonds, with the amino acid side chains extending outward from the exterior surface of the helix. Amphiphilic helices, in which apolar residues occupy one face of the helix and more polar residues are located on the other face, have surfactant properties and spontaneously assemble in aqueous solution to minimize the exposure of the hydrophobic surface to the solvent and to present the hydrophilic surface to the aqueous environment.

In the present paper, we have applied the principles of protein design to create a peptide, denoted nano-1, that folds into an amphiphilic α-helix and coats carbon nanotubes. The hydrophobic face of the helix was intended to interact noncovalently

† Department of Chemistry, The University of Texas at Dallas.
‡ NanoTech Institute, The University of Texas at Dallas.
§ Department of Molecular and Cell Biology, The University of Texas at Dallas.
|| Zyvex Corporation.

(1) Dresselhaus, M. S.; Dresselhaus, G.; Avouris, P., Eds. *Carbon Nanotubes: Synthesis, Structure, Properties, and Applications*; Springer: New York, 2001; Vol. 80.
(2) Tans, S. J.; Verschueren, A. R. M.; Dekker, C. *Nature* **1998**, *393*, 49−52.
(3) Hu, J. T.; Min, O. Y.; Yang, P. D.; Lieber, C. M. *Nature* **1999**, *399*, 48−51.
(4) Fan, S. S.; Chapline, M. G.; Franklin, N. R.; Tombler, T. W.; Cassell, A. M.; Dai, H. J. *Science* **1999**, *283*, 512−514.
(5) Baughman, R. H.; Cui, C. X.; Zakhidov, A. A.; Iqbal, Z.; Barisci, J. N.; Spinks, G. M.; Wallace, G. G.; Mazzoldi, A.; De Rossi, D.; Rinzler, A. G.; Jaschinski, O.; Roth, S.; Kertesz, M. *Science* **1999**, *284*, 1340−1344.
(6) Baughman, R. H.; Zakhidov, A. A.; de Heer, W. A. *Science* **2002**, *297*, 787−792.
(7) Kohn, W. D.; Mant, C. T.; Hodges, R. S. *J. Biol. Chem.* **1997**, *272*, 2583−2586.

10.1021/ja029084x CCC: $25.00

with the aromatic surface of carbon nanotubes, and the hydrophilic face was designed to promote self-assembly through charged peptide-peptide interactions. Endowing SWNTs with the peptide surface reported here disperses the nanotubes in an aqueous medium and, more significantly, facilitates the regulated self-assembly of the peptide-coated nanotubes into structures of different sizes and shapes by controlling factors that affect peptide−peptide interactions.

Experimental Section

Molecular Modeling. The methods used for the mathematical generation of helical peptide structures associated with (8,8) carbon nanotubes (metallic nanotubes with a 10.8 Å diameter) are similar to those described previously in the modeling of helical peptide ion channels.[8] Model building and energy refinement calculations were performed using InsightII and Discover (Accelrys Inc., San Diego, CA). Coordinates for an (8,8) carbon nanotube were obtained from The Nanotube Site[9] and replicated to generate an individual nanotube 96 Å in length (1264 atoms). An idealized helix was built, using the backbone dihedral angles $\phi = -65°$ and $\psi = -40°$, with the nano-1 sequence Ac-E(VEAFEKK)(VAAFESK)(VQAFEKK)(VEAFEHG)-$CONH_2$ (Ac indicates N-terminal acetylation, $CONH_2$ indicates C-terminal amidation, and single letter symbols for each amino acid are used[10]). Each phenylalanine (Phe) side chain was placed in a favorable rotamer position with $\chi_1 = -150°$ and $\chi_2 = 140°$. The helix was transformed to 3.5 residues per turn using a matrix transformation (eq 1 in ref 11) with a superhelical pitch (p) of −189 Å. Six copies of the nano-1 helix were placed at the corners of a regular hexagon with sides of 12 Å (the interhelical distance), with each helix rotated to position the a and d residues[12] toward the hexagon center. The 6-helix bundle was then given a left-handed twist using eq 1 from ref 11 with a p value of 320 Å. The backbone dihedral angles of the four C-terminal residues of each helix were adjusted to the values observed in the crystal structure of $CoilV_aL_d$[13] to accommodate head-to-tail interactions between helices. A second copy of the 6-helix bundle was then created and displaced by 43 Å and rotated by 13°, both about the bundle axis, to generate six head-to-tail helix dimers with hydrogen-bonding interactions in the backbone between the N- and C-termini of the two helices in each dimer. One copy of the nanotube was centered in the 12-helix aggregate, and a 5 Å wide shell of water molecules was added to surround the entire system. The resulting model was subjected to energy minimization using Discover and the Consistent Valence Force Field (CVFF),[14] with the force field parameters for sp^2-hybridized carbon used for the carbon atoms of the nanotube. The positions of all atoms in the system were allowed to change (unrestrained) during the energy refinement.

Peptide Synthesis and Purification. Nano-1 was synthesized at a 0.1 mmol scale on an Applied Biosystems 433A solid-phase peptide synthesizer equipped with an Alltech model 450 UV detector using 9-fluorenylmethoxycarbonyl (Fmoc)-protected amino acids and standard solid-phase peptide synthetic methods.[15] The resin used was ABI Fmoc-amide resin, which produces an amide-protected C-terminus upon cleavage of the peptide from the resin. The N-terminus of the peptide was acetylated prior to cleavage. Cleavage and side chain deprotection was effected using a 9:0.5:0.3:0.2 trifluoroacetic acid (TFA):thioanisole:ethanedithiol:anisole mixture. Crude peptide was precipitated using cold diethyl ether, lyophilized, and purified using reversed-phase HPLC and Vydac C4 columns with water/acetonitrile/0.1% TFA mobile phase gradients. The identity of the peptide was verified using electrospray ionization mass spectrometry.

Peptide/Nanotube Sample Preparations. Peptide samples were prepared at the desired concentration by diluting a stock amount with deionized water. Peptide concentration was determined by measuring the absorbance at 260 nm ($\epsilon = 788$ L mol^{-1} cm^{-1}). As-synthesized SWNTs produced by the method of high-pressure decomposition of carbon monoxide (HiPco process)[16] were purchased from Carbon Nanotechnologies Inc, lot # Hpr 86; as-synthesized SWNTs produced by pulsed laser vaporization (PLV)[17] were purchased from Tubes@Rice. HiPco SWNTs have a diameter distribution between 0.7 and 1.4 nm with an average diameter of approximately 1.1 nm. SWNTs produced using the PLV methods are on average larger diameter tubules with an average diameter of approximately 1.3 nm. The dominant impurity in both cases is metal catalyst, which is encased in thin carbon shells and distributed throughout the sample as 3 to 5 nm diameter particles. In HiPco SWNTs, the raw sample typically contains in excess of 15 wt % catalyst. In the case of PLV SWNTs, Co and Ni are used as catalyst and are typically 7 to 10 wt %. Approximately 0.15 mg of SWNTs (HiPco or PLV) were placed on the surface of 3 mL of peptide solution. Sonication was performed using a Sonics & Materials, Inc. (Newton, CT) model VC-50 Vibra Cell sonicator equipped with a 4 mm diameter micro tip. The tip was placed into the sample approximately one-third of the distance from the surface and sonicated for 1 min per mL of sample (up to two minutes) at a power level of 12 to 15 W. Samples were then centrifuged in an Eppendorf microcentrifuge for 5 min at 14 000 rpm. The upper 75% of the supernatant was recovered from the centrifugation tubes using a small-bore pipet, avoiding sediment at the bottom, transferred to a clean vial, and used in further experiments.

Salted nano-1/SWNT samples were prepared by additions from a 1.0 M NaCl stock solution to 1.0 mL of a peptide (100 μM)/SWNT dispersion to yield solutions at the desired NaCl concentration. All volume additions were smaller than 5% of the original dispersion volume.

Scanning Electron Microscopy (SEM). SEM images were acquired using a LEO 1530 field-emission scanning electron microscope at an accelerating voltage of 1 keV. One drop of the nano-1/nanotube solution was placed on a pre-cleaned Si chip or a carbon substrate. Most of the solvent was then wicked

(8) Dieckmann, G. R.; Lear, J. D.; Zhong, Q. F.; Klein, M. L.; DeGrado, W. F.; Sharp, K. A. *Biophys. J.* **1999**, *76*, 618−630.
(9) http://www.pa.msu.edu/cmp/csc/nanotube.html.
(10) Voet, D.; Voet, J. G. *Biochemistry*, 2 ed.; John Wiley & Sons: New York, 1995.
(11) Dieckmann, G. R.; McRorie, D. K.; Lear, J. D.; Sharp, K. A.; DeGrado, W. F.; Pecoraro, V. L. *J. Mol. Biol.* **1998**, *280*, 897−912.
(12) Mclachlan, A. D.; Stewart, M. *J. Mol. Biol.* **1975**, *98*, 293−304.
(13) Ogihara, N. L.; Weiss, M. S.; DeGrado, W. F.; Eisenberg, D. *Protein Sci.* **1997**, *6*, 80−88.
(14) Dauber-Osguthorpe, P.; Roberts, V. A.; Osguthorpe, D. J.; Wolff, J.; Genest, M.; Hagler, A. T. *Proteins* **1988**, *4*, 31−47.
(15) Bodanszky, M. *Peptide Chemistry: A Practical Approach*, 2 ed.; Springer-Verlag: New York, 1993.
(16) Nikolaev, P.; Bronikowski, M.; Bradley, R.; Rohmund, F.; Colbert, D.; Smith, K.; Smalley, R. *Chem. Phys. Lett.* **1999**, *313*, 91−97.
(17) Thess, A.; Lee, R.; Nikolaev, P.; Dai, H. J.; Petit, P.; Robert, J.; Xu, C. H.; Lee, Y. H.; Kim, S. G.; Rinzler, A. G.; Colbert, D. T.; Scuseria, G. E.; Tomanek, D.; Fischer, J. E.; Smalley, R. E. *Science* **1996**, *273*, 483−487.

away using a Kimwipe. The Si chip or carbon substrate was completely dried in the air before SEM measurements were conducted. No metal coating was used for the samples. Energy-dispersive X-ray spectrometry (EDS) was carried out at an accelerating voltage of 20 keV using an Oxford INCA system interfaced with the SEM instrument. The system uses a Si(Li) detector, cooled by liquid nitrogen, which has an energy resolution of 129 eV.

Transmission Electron Microscopy (TEM). TEM images were acquired using a JEOL 2000FX transmission electron microscope at an accelerating voltage of 120 kV. One drop of the nano-1/nanotube solution was placed on a 400 mesh Cu TEM grid with a holey carbon support film (SPI Supplies) in contact with a Kimwipe. The solvent was quickly wicked away, preventing the aggregation of nanotubes. The TEM grid was completely dried in the air before TEM measurements were conducted.

Circular Dichroism (CD) Spectroscopy. CD spectral measurements were made at 25 °C using an Aviv model 202 circular dichroism spectrometer and a 1 mm path length rectangular quartz cuvette. Spectra were collected from 190 to 260 nm at 1 nm intervals and averaged for 6 s at each wavelength.

Raman Spectroscopy. All Raman spectra were recorded on a Jobin Yvon Horiba high-resolution LabRam Raman microscope system, which contains an optical microscope adapted to a double grating spectrograph and a CCD array detector. The laser excitation was provided by a Spectra-Physics model 127 helium−neon laser operating at 35 mW of 633 nm output. The laser power at the sample was ~8 mW and was focused to ~1 μm. Spectra were recorded by scanning the 50 to 3000 cm^{-1} region with a total acquisition time of 8 min. Wavenumber calibration was carried out using the 520.5 cm^{-1} line of a silicon wafer. A spectral resolution of ~1 cm^{-1} was used. For polarized Raman studies, the spectrum parallel to the microfiber, $\alpha = 0°$, was measured with the plane of the laser and the analyzer horizontal and parallel to the microfiber. The spectrum perpendicular to the microfiber, $\alpha = 90°$, was measured after rotation of the microfiber by 90°. Samples were aligned by rotating the support until it was judged either parallel or perpendicular to the plane of the laser. Spectra were fit with Lorentzian functions by searching for the minimum number of frequencies that fit the different bands equally well without fixing the positions and widths of the individual peaks.

Thermogravimetric Analysis (TGA). The maximum solubility of SWNTs in an aqueous 100 μM nano-1 solution was determined from a nano-1/HiPco SWNT dispersion saturated with SWNTs. The resulting solution was frozen using liquid nitrogen and lyophilized. TGA measurements were made using a Perkin-Elmer Pyris 1 thermogravimetric analyzer in an oxygen atmosphere. The weight fractions of the SWNTs and the peptide were obtained from the burning curve.

Results

Peptide Design and Modeling. The amino acid sequence of an amphiphilic helix contains a repeating heptad designated $(a\ b\ c\ d\ e\ f\ g)_n$, where *a* through *g* refer to the positions in the linear sequence.[12] When folded into an α-helix, hydrophobic residues in positions *a* and *d* will generate an apolar face of the helix, whereas more hydrophilic residues in the other positions will form a more polar surface. We designed a 29-residue peptide, denoted nano-1 (sequence shown in Figure 1), to form an amphiphilic α-helix based on the previously characterized peptide $CoilV_aL_d$.[13] Specific design features of nano-1 include: (1) the *a* and *d* positions of each heptad are occupied by the hydrophobic residues valine (Val) and Phe, respectively. Phe, being aromatic, should interact effectively with the nanotube surface similar to the pyrene-based bifunctional cross-linking agent used previously by Dai and co-workers to noncovalently attach proteins to nanotubes.[18] Phe in the *d* positions should also disfavor peptide aggregation and promote peptide/nanotube association by disrupting the helix-helix packing surface of the native $CoilV_aL_d$ sequence upon which nano-1 is based; (2) polar residues are located in positions *e* and *g* to generate favorable helix−helix interactions once peptides associate with nanotubes; (3) oppositely charged polar residues are placed in positions *b* and *f* to provide favorable interactions between helices from different peptide/nanotube complexes, as observed in the crystal structures of other amphiphilic helices.[19] The strength of the ionic interactions between charged residues in peptides coating adjacent nanotubes can then be modulated by changing the solution ionic strength; (4) the N- and C-termini of the peptide are acetylated and amidated, respectively, to remove charges from the termini, making the peptide less polar and increasing its affinity for carbon nanotubes. The absence of terminal charges should also allow formation of parallel helical aggregates (the N- and C-termini of all helices oriented in the same directions) without repulsions from similarly charged peptide termini. An unrestrained energy-minimized model of the interaction of nano-1 with a typical (8,8) SWNT of diameter 10.8 Å reveals that six nano-1 α-helices are sufficient to surround the circumference of an individual SWNT, while maintaining typical interhelical interactions (Figure 2A). Furthermore, head-to-tail stacking of the helices through backbone hydrogen bonding between the N-terminus of one helix and the C-terminus of a second helix (as observed in the crystal structure of $CoilV_aL_d$[13]) would allow for wrapping of a SWNT along its entire length (Figure 2B).

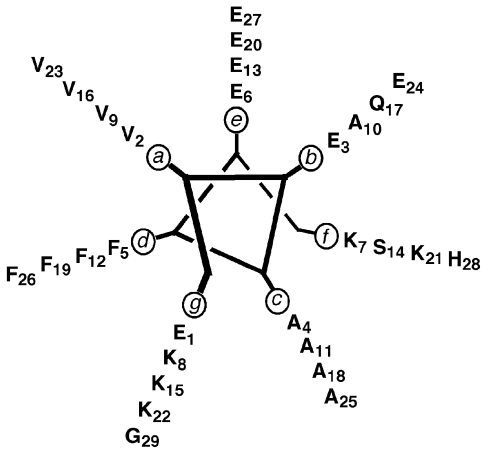

Figure 1. Helical wheel diagram showing positions of residues in the α-helix. The nano-1 sequence is Ac-E(VEAFEKK)(VAAFESK)(VQAFEKK)-(VEAFEHG)-$CONH_2$, where Ac indicates acetylation of the N-terminus, $CONH_2$ indicates amidation of the C-terminus, and the parentheses denote heptad repeats.

(18) Chen, R. J.; Zhang, Y.; Wang, D.; Dai, H. *J. Am. Chem. Soc.* **2001**, *123*, 3838−3839.
(19) Prive, G. G.; Anderson, D. H.; Wesson, L.; Cascio, D.; Eisenberg, D. *Protein Sci.* **1999**, *8*, 1400−1409.

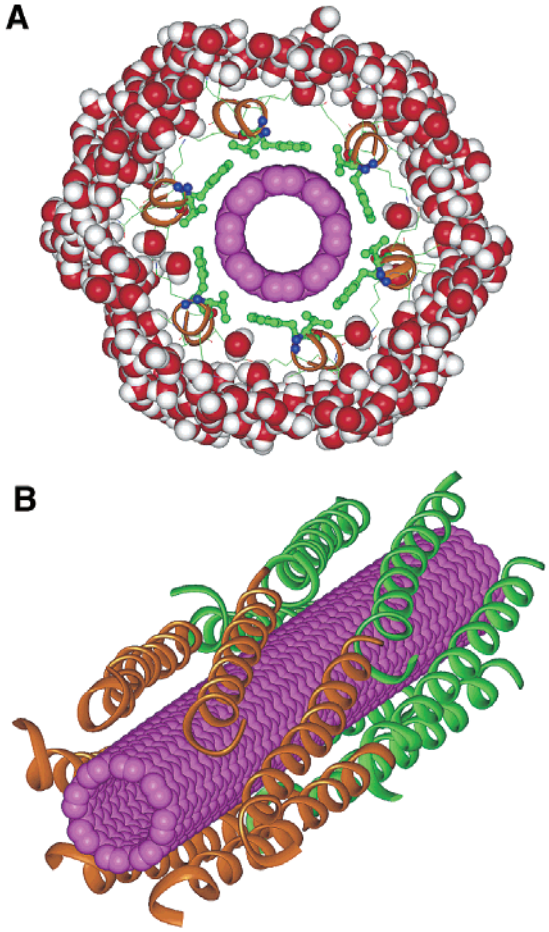

Figure 2. Model illustrating potential interactions between nano-1 and SWNT. (**A**) Cross-section view of a SWNT (pink cylinder) wrapped by six peptide helices (one heptad of each shown). The backbone of each peptide is denoted by an orange ribbon, and the Val and Phe side chains packed against the SWNT surface are rendered in green. The 5 Å thick water shell used in the energy refinement of the model is rendered as CPK spheres (red = oxygen, white = hydrogen, green = carbon, blue = nitrogen). (**B**) View of peptide-wrapped nanotube illustrating the 12 peptide helices used in the model. The head-to-tail alignment of helices in two adjacent layers (orange and green layers) is maintained throughout the simulation. The unwinding observed at the C-terminus of each helix was manually introduced at the beginning of the simulation to mimic the distortion observed in the crystal structure of $CoilV_aL_d$.

Interaction of Nano-1 with SWNTs. The secondary structure of nano-1 in aqueous solution, in the presence and absence of carbon nanotubes, was investigated by CD. At 100 μM peptide, there were no prominent negative CD peaks indicative of α-helical secondary structure; however, at 200 μM, there were conspicuous peaks at 208 and 222 nm, signatures of α-helical structure (Figure 3). Thus, nano-1 adopts an α-helical conformation in aqueous solution as a function of peptide concentration, suggesting that the helical fold is stabilized by hydrophobic contacts between the *a*/*d* faces of two or more peptides that associate at higher peptide concentrations, as expected from the amphiphilic design of the peptide. As-synthesized SWNTs produced by both the HiPco process[16] and by pulsed laser vaporization[17] are insoluble in water. However, when sonicated in the presence of 100 μM nano-1 in water, both HiPco (Figure 4A) and PLV (data not shown) nanotubes dispersed to form homogeneous black solutions. The CD spectrum of the dispersion made by sonicating HiPco SWNTs in the presence of 100 μM aqueous nano-1 displayed prominent negative signals at 208

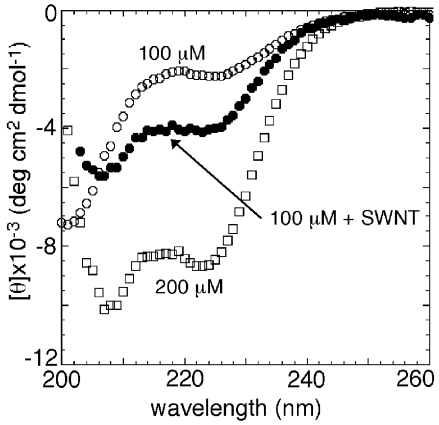

Figure 3. CD spectra of nano-1 in water at 100 μM (open circles), at 200 μM (open squares), and at 100 μM sonicated in the presence of SWNTs (filled circles).

and 222 nm, indicating an increase in the helical content of nano-1 (Figure 3). This observation suggests that the α-helical conformation of the peptide is stabilized in the presence of the nanotubes through hydrophobic interactions between the peptide *a*/*d* face and the nanotube surface. The nano-1/SWNT dispersion is stable at room temperature for at least 12 weeks. To determine the maximum solubility of HiPco SWNTs in an aqueous 100 μM nano-1 solution, a dispersion saturated with SWNTs was prepared and analyzed by TGA. The nanotube solubility (not counting catalyst) was determined to be 0.7 mg mL^{-1}.

Optical and electron microscopy were used to characterize the nano-1/nanotube composites. Low-resolution transmission electron microscopy (TEM) of a nano-1/SWNT dispersion dried on a TEM grid revealed an extensive network of ~10 nm diameter microfibrils coated with a web-like film (Figure 4B). This coating is similar to that observed in SDS-solubilized SWNT solutions.[20] High-resolution TEM of the microfibrils in the network showed bundles of SWNTs that are highly aligned with the microfibril axis (Figure 4C). A similar nanotube alignment was observed in nano-1/PLV SWNT dispersions (data not shown). The nano-1/SWNT dispersion was diluted 10-fold with distilled water to investigate the importance of peptide concentration on the formation of the peptide/nanotube network. Upon dilution, large fibrillar structures slowly form and settle out of the solution; optical microscopy revealed fibrillar structures of ~10 μm in diameter that appear to be composed of smaller microfibers with 2 μm diameters (Figure 4D). This fibrillar solid can be resuspended by the addition of nano-1, followed by sonication. When the same nano-1/SWNT dispersion is diluted 10-fold with a 100 μM nano-1 solution instead of distilled water, no solid forms. These observations suggest that an equilibrium exists in solution between free peptide and peptide associated with SWNTs.

Raman spectroscopy was used to further probe the structure of peptide/nanotube fibers. A prominent feature in the Raman spectrum of SWNTs is the radial breathing mode in the 160 to 300 cm^{-1} region associated with a symmetric movement of all carbon atoms in the radial direction. Using various energies of the incident laser beam, specific tube resonant enhancements are observed for these modes that are a consequence of the one-dimensional nature of SWNTs and the existence of singularities

(20) Bonard, J. M.; Stora, T.; Salvetat, J. P.; Maier, F.; Stockli, T.; Duschl, C.; Forro, L.; De Heer, W. A.; Chatelain, A. *Adv. Mater.* **1997**, *9*, 827−831.

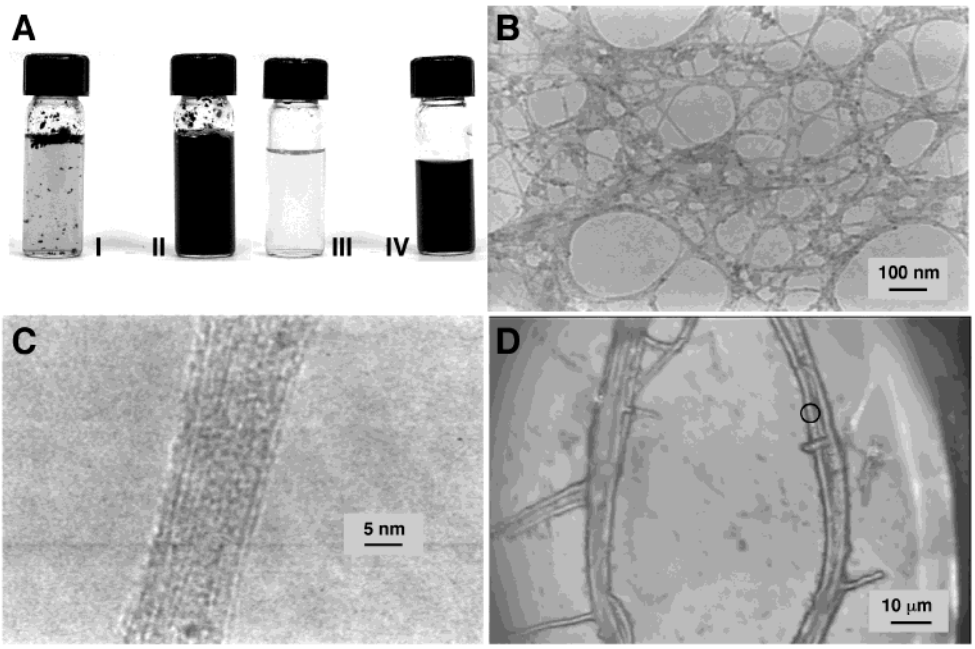

Figure 4. Optical and electron microscopy of nano-1/nanotube composites. (**A**) Photographs of vials showing HiPco SWNTs in water (**I**) and in nano-1 solution (**II**) after sonication, and the same two solutions after filtration (**III** and **IV**). (**B**) Low-resolution TEM image of solution **IV** in **4A** showing coating of nanotube fibers by nano-1. The small dark spheres are Fe catalyst particles from the HiPco SWNT synthesis. (**C**) High-resolution TEM image showing the alignment of individual SWNTs in the bundles (HiPco sample). (**D**) Optical micrograph of the fibers and microfibers that form within 36 h from the nano-1/nanotube solution after 10-fold dilution with distilled water. The circled area indicates the location where polarized Raman measurements were made.

in their density of states.[21] The frequency and modal distribution of the radial breathing modes depend primarily on the diameter and chirality of the nanotubes, and whether the nanotubes directly contact one another in bundles.[22,23] To determine if nano-1 coats and separates nanotubes, we measured the Raman spectra for SWNTs and nano-1/SWNT dispersions in the 160 to 300 cm^{-1} region and looked for increases in the frequencies of the radial breathing modes, analogous to those observed when nanotubes are debundled and coated by conjugated organic polymers.[24] For PLV SWNTs, the radial breathing mode feature has a narrow full width at half-maximum with a dominant peak centered at 190 cm^{-1} (Figure 5A). This observation is consistent with previous studies on these types of nanotubes and indicates a narrow diameter distribution. After the nanotubes were dispersed in aqueous solution by sonication with nano-1, there was a shift to higher frequencies in the radial breathing mode by more than 9 cm^{-1} (Figure 5B), evidence that the nanotubes were no longer in direct contact with one another along their length as they were in the absence of peptide. Shown in Figure 5C are peaks associated with the radial breathing modes for HiPco nanotubes. There are multiple peaks due, in part, to heterogeneity in the diameters of the nanotubes produced by this process. After the HiPco nanotubes were sonicated with nano-1, there was again an increase in the frequency for each of these peaks, strongly suggesting that the peptide intercalates between the nanotubes in the raw material, coating, and separating the nanotubes (Figure 5D). It should be noted that in the radial breathing mode region there are no prominent Raman active modes for the peptide. The argument that peptide is coating individual nanotubes is further strengthened by

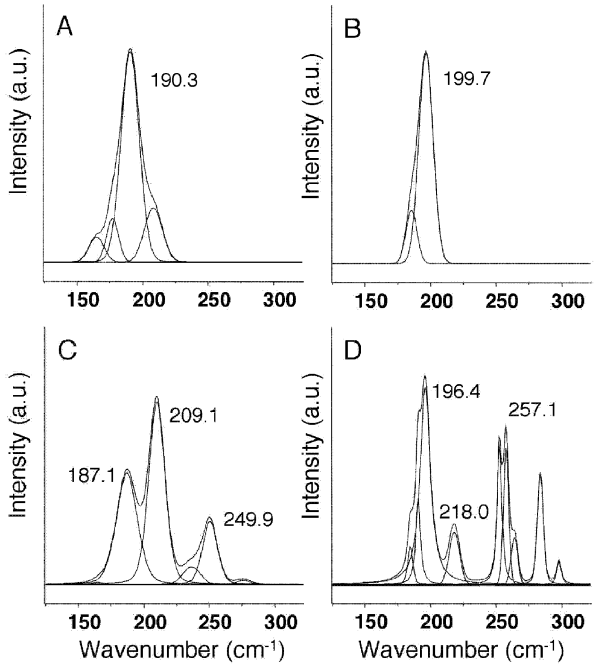

Figure 5. Raman spectroscopic analysis of SWNTs and nano-1/SWNT dispersions. (**A**) and (**B**) show the radial breathing mode features for SWNT produced using PLV for the raw powder (**A**) and nano-1/SWNT dispersion (**B**). The number of Lorentzian components are reduced in the dispersion with an overall upshift of 9 cm^{-1} for the main feature. Similarly, (**C**) and (**D**) show the radial breathing mode features for SWNT produced using the HiPco method for the raw product (**C**) and the nano-1/SWNT dispersion (**D**).

(21) Dresselhaus, M. S.; Dresselhaus, G.; Eklund, P. C. *Science of Fullerenes and Carbon Nanotubes*; Academic Press: New York, 1996.
(22) Jishi, R. A.; Venkataraman, L.; Dresselhaus, M. S.; Dresselhaus, G. *Chem. Phys. Lett.* **1993**, *209*, 77−82.
(23) Saito, R.; Takeya, T.; Kimura, T.; Dresselhaus, G.; Dresselhaus, M. S. *Phys. Rev. B* **1998**, *57*, 4145−4153.
(24) Dalton, A. B.; Stephan, C.; Coleman, J. N.; McCarthy, B.; Ajayan, P. M.; Lefrant, S.; Bernier, P.; Blau, W. J.; Byrne, H. J. *J. Phys. Chem. B* **2000**, *104*, 10 012−10 016.

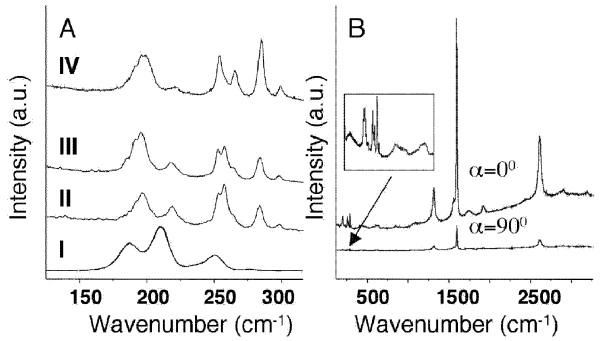

Figure 6. Raman spectroscopic analysis of nano-1/SWNT composites. **(A)** Comparison of the Raman spectra of (**I**) HiPco SWNTs, (**II**) stable dispersion of SWNTs in aqueous peptide solution, (**III**) dispersion precipitate after addition of NaCl, and (**IV**) fibrillar structure formed after 10-fold dilution with distilled water. (**B**) Polarized Raman spectra of nano-1/SWNT precipitate shown in Figure **4D**. In the case where $\alpha = 0°$, the incident laser beam is polarized parallel to the axis of the fiber. For $\alpha = 90°$, the incident laser beam is polarized perpendicular to the fiber axis. The inset expands the radial-breathing modes at $\alpha = 90°$, showing that they are present but greatly reduced in intensity.

changes observed in the nanotube tangential mode feature centered at 1590 cm^{-1} in the case of the peptide/SWNT composite. As is observed for nanotubes debundled by conjugated polymers,[24] the tangential mode feature narrows and undergoes an apparent increase in frequency of $\sim$4 cm^{-1} (data not shown).

Figure 6A compares the radial breathing modes of raw HiPco nanotubes with nano-1/SWNT composites produced under different conditions. The spectra include those for nanotubes alone (I), peptide/nanotube dispersions made in aqueous solution in the absence of salt (II) and after the addition of 100 mM NaCl (III), and the fibrillar structures that aggregate upon dilution of the dispersion with water (IV). Each of the conditions under which peptide/nanotube composites were produced resulted in material that had similar increases in the radial breathing mode frequencies, suggesting that peptide had coated and separated the nanotubes. Due to the relatively efficient scattering associated with SWNTs in the radial breathing mode region of the spectrum, it was not possible to distinguish any modes associated with the peptide. However, peptide modes are observed elsewhere in the spectrum. For example, a tangential C−N stretch is observed in the 400 to 500 cm^{-1} frequency region of the peptide/nanotube material (two broad bands on right side of inset in Figure 6B). Interestingly, the shape of this feature is modified in the presence of SWNTs. We are presently conducting a more extensive Raman investigation of the peptide/SWNT system.

On the basis of the peptide design, it is expected that fibrils made from peptide-coated nanotubes would induce orientation of SWNTs within the solidified matrix. To this end, orientation-dependent measurements were performed using polarized Raman scattering. Figure 6B displays a Raman spectrum for the microfibers in Figure 4D, between 250 and 3000 cm^{-1}, for angles $\alpha = 0°$ and $\alpha = 90°$ between the polarization direction of the incident excitation and the microfiber axis. The modes associated with SWNTs show maximum intensity at $\alpha = 0°$. However, when the sample is excited with the polarization orthogonal to a microfiber axis ($\alpha = 90°$), the intensity is conspicuously reduced. These data indicate that the nanotubes are highly oriented along the axis of the microfibers.

Controlled Assembly of Peptide-Coated SWNTs. The self-assembly properties of the peptide nano-1 were used to control the size and morphology of peptide/SWNT fibers. Nano-1 was designed so that favorable charge−charge interactions would occur among peptides coating the exterior surfaces of separate nanotubes, leading to oligomerization of the peptide-coated nanotubes into higher-order structures. Similar peptide−peptide interactions have been observed in the crystal structure of a 12-residue amphiphilic helical peptide, which assembles into extended helical bundle sheets.[19] The strength of the charge−charge interactions, and hence the formation of higher-order structures, was manipulated by controlling the ionic strength of the aqueous solution through addition of NaCl. Salts are used routinely to aid in protein crystallization by screening local charges on protein surfaces.[25] The addition of increasing concentrations of NaCl to dispersions formed by the sonication of HiPco nanotubes in the presence of 100 μM nano-1 caused the peptide-coated nanotubes to visibly assemble into larger structures, and the extent of aggregation was a function of the NaCl concentration (data not shown). SEM was used to compare features of the assembled material at different salt concentrations (Figure 7). In the absence of NaCl, small fibers with widths of 100 ± 15 nm (n = 20) were evident (Figure 7A). At progressively higher salt concentrations, the diameter of the peptide/nanotube fibers increased dramatically, with widths of 22 ± 5 μm (n = 12) and 38 ± 8 μm (n = 14) observed at 40 mM (Figure 7B) and 120 mM NaCl (Figure 7C), respectively. EDS spectra of these large fibers (Figure 7B and 7C) revealed the presence of Fe (data not shown), evidence that the fibers contained carbon nanotubes; HiPco SWNTs are associated with Fe nanoparticles derived from the catalyst employed in the manufacturing of the nanotubes. Raman spectra of NaCl-induced fibers (Figure 6A, spectrum III) confirmed the presence of carbon nanotubes in the fibers and showed increases in the radial breathing mode frequencies similar to those observed for peptide-coated nanotubes in the absence of salt (Figure 6A, spectra II and IV), suggesting that the fibers were composed of peptide-coated SWNTs. We conclude from these data that the self-assembly of peptide-coated nanotubes can be controlled by salt concentration to produce fibers of different diameters.

Solution conditions other than the concentration of salt can be manipulated to regulate the self-association of proteins. For example, amphiphilic molecules modify the crystal formation of peptides and proteins by selectively interacting with one or more specific surfaces of a growing crystal, apparently because the amphiphilic molecules suppress hydrophobic interactions and improve packing density in the solid state.[26−28] Therefore, we investigated the possibility that an amphiphilic additive would influence the type of oligomers formed by peptide-coated nanotubes. *N*,*N*-dimethylformamide (DMF) was added to the nano-1/SWNT dispersion at a concentration of 0.0015 vol %. The addition of DMF did not cause immediate oligomerization, but a solid did appear in the solution within 24 h; this result is in contrast to the instantaneous formation of precipitate that is

(25) Bonnete, F.; Malfois, M.; Finet, S.; Tardieu, A.; Lafont, S.; Veesler, S. *Acta Crystallogr. D* **1997**, *53*, 438−447.
(26) Miegel, A.; Sano, K.; Yamamoto, K.; Maeda, K.; Maeda, Y.; Taniguchi, H.; Yao, M.; Wakatsuki, S. *FEBS Lett.* **1996**, *394*, 201−205.
(27) Hamana, H.; Moriyama, H.; Shinozawa, T.; Tanaka, N. *Acta Crystallogr. D* **1999**, *55*, 345−346.
(28) Tanaka, S.; Ataka, M.; Kubota, T.; Soga, T.; Homma, K.; Lee, W. C.; Tanokura, M. *J. Crystal Growth* **2002**, *234*, 247−254.

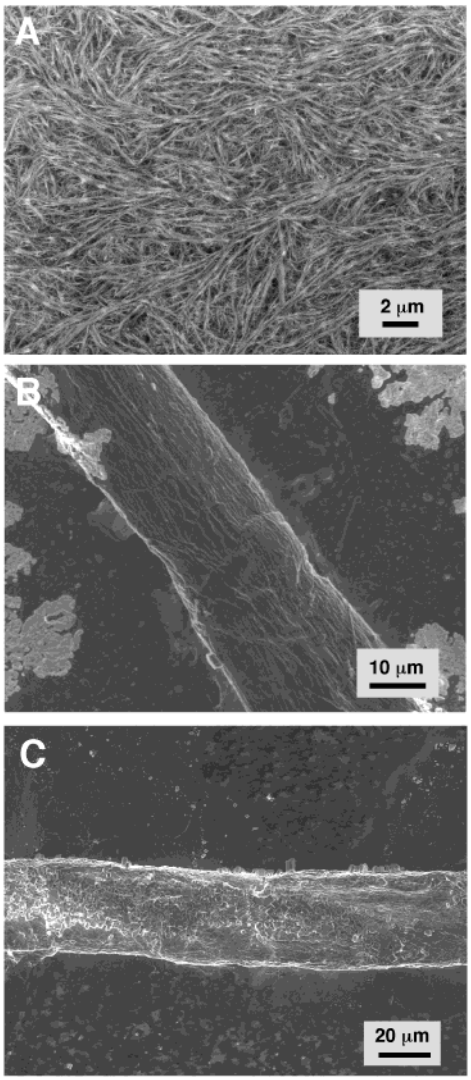

Figure 7. SEM images of nano-1/SWNT fibers formed from a 100 μM peptide/nanotube dispersion upon addition of no salt (**A**), 40 mM NaCl (**B**), and 120 mM NaCl (**C**).

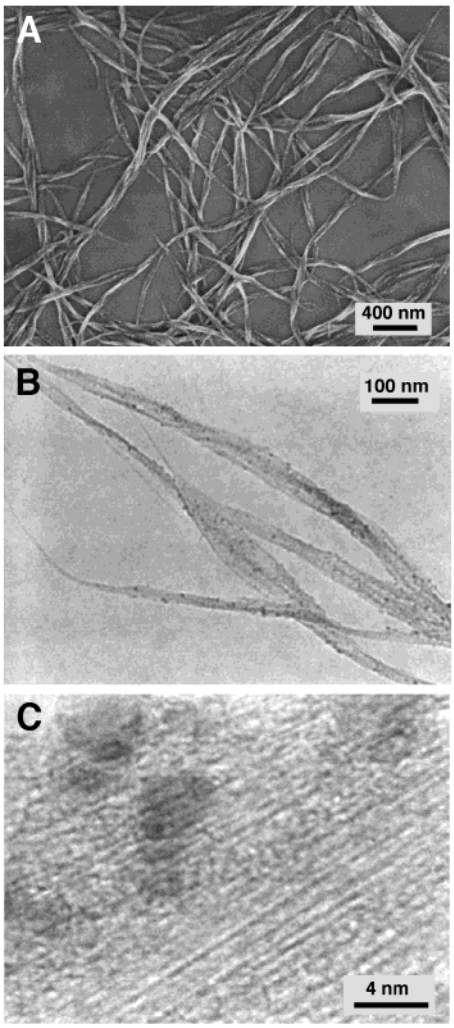

Figure 8. (**A**) SEM image of fibers formed from the addition of 0.0015% (by volume) DMF to a nano-1/SWNT dispersion. (**B**) Low-resolution TEM image of the same fibers observed in **8A**. The small dark spheres are Fe catalyst particles from the HiPco SWNT synthesis. (**C**) High-resolution TEM image of the same fibers showing alignment of nanotubes. The large dark areas are Fe particles.

observed when NaCl is added to the peptide/SWNT dispersion. The solid formed from the addition of DMF was composed of interwound long strands, as observed by SEM (Figure 8A). Low-resolution TEM imaging revealed that the strands were thin ribbon-like fibrils 30 to 75 nm wide (Figure 8B). The extensive alignment of the nanotubes in the fibrils is evident in the high-resolution TEM images (Figure 8C). The change in morphology from cylindrical microfibers (no DMF) to flat ribbons suggests a selective interaction between the DMF and the peptide/SWNT composite. Altogether, these data demonstrate that nanotubes coated with nano-1 can be induced to assemble into higher order structures and that the type of structure (i.e., cylindrical microfiber or flat ribbon) can be controlled by the addition of either salt or the amphiphilic additive DMF.

Discussion

Two challenges facing the carbon nanotube field are the dispersion of nanotubes in solution and their assembly into useful structures. Previous strategies for solubilizing SWNTs without covalent modification include the use of organic solvents,[29] detergents,[30] natural polysaccharides such as gum Arabic[31] and amylose,[32] and organic polymers.[24,33,34] Although these approaches increase the solubility of SWNTs, they have not been generally adapted to control the assembly of solubilized SWNTs into higher order structures. In the present paper, we have used amphiphilic α-helical peptides to not only coat and solubilize SWNTs, but also to regulate the reassembly of the peptide coated nanotubes into supramolecular structures by controlling the factors that influence peptide−peptide interactions.

Sonication of SWNTs in an aqueous solution of nano-1 solubilized the nanotubes to form a stable dispersion. CD

(29) Bahr, J. L.; Mickelson, E. T.; Bronikowski, M. J.; Smalley, R. E.; Tour, J. M. *Chem. Commun.* **2001**, 193−194.
(30) Bandow, S.; Rao, A. M.; Williams, K. A.; Thess, A.; Smalley, R. E.; Eklund, P. C. *J. Phys. Chem. B* **1997**, *101*, 8839−8842.
(31) Bandyopadhyaya, R.; Nativ-Roth, E.; Regev, O.; Yerushalmi-Rozen, R. *Nano Lett.* **2002**, *2*, 25−28.
(32) Star, A.; Steuerman, D. W.; Heath, J. R.; Stoddart, J. F. *Angew. Chem., Int. Ed.* **2002**, *41*, 2508−2512.
(33) O'Connell, M. J.; Boul, P.; Ericson, L. M.; Huffman, C.; Wang, Y.; Haroz, E.; Kuper, C.; Tour, J.; Ausman, K. D.; Smalley, R. E. *Chem. Phys. Lett.* **2001**, *342*, 265−271.
(34) Chen, J.; Liu, H.; Weimer, W. A.; Halls, M. D.; Waldeck, D. H.; Walker, G. C. *J. Am. Chem. Soc.* **2002**, *124*, 9034−9035.

measurements revealed that the nanotubes induced the peptide to fold into an α-helical structure, evidence that the helical conformation is stabilized by interactions of the hydrophobic face of the helix with the nanotube surface. Stabilization of the helical peptide conformation by hydrophobic interactions is also consistent with the observation that the α-helical content of nano-1 in the absence of nanotubes increased as a function of peptide concentration. These data are consistent with nano-1 performing according to design specifications; that is, the peptide folded into an amphiphilic α-helix and strongly interacted with the hydrophobic surface of SWNTs via the hydrophobic face of the peptide helix.

The extent to which nano-1 coated and debundled SWNTs was studied by Raman spectroscopy of the nanotube radial breathing modes. Both theoretical and experimental work has shown that the frequency of the radial breathing mode is inversely proportional to the diameter of individual nanotubes.[22,23] In nanotube aggregates, it has been postulated that there is a weak inter-tubule coupling via van der Waals interactions that manifests itself as a 6 to 20 cm^{-1} shift to higher frequencies due to the space restrictions imposed by neighboring tubes.[35] However, a recent study comparing organic dispersions of shortened nanotubes, containing either individual tubes or small ropes and bundles from raw material, revealed an increase in the radial breathing mode position in the debundled dispersion relative to the raw material.[36] This apparent contradiction to lattice dynamics predictions was attributed to a decreased energy spacing of the singularities in the density of states in isolated tubes compared to that in bundles. As the resonant absorptions of SWNTs in these samples were modified, the same laser excitation wavelength probed different nanotubes, resulting in a spectrum with distinct changes in the radial breathing mode frequencies and modal distribution. In addition, SWNTs dispersed in organic suspensions of conjugated polymer have an increase in the radial breathing mode frequencies associated with exfoliation and intercalation of the polymer into nanotube aggregates.[24] Thus, if nano-1 coats and debundles SWNTs, an increase in the frequency of the radial breathing mode peaks, compared to bundled nanotubes, would be expected, and we observed an increase of over 9 cm^{-1}. This evidence is consistent with nano-1 intercalating between a large percentage of the nanotubes in bundles coating them with peptide.

Sonicating SWNTs with nano-1 in the absence of salt or other additives produced a reticulum of interconnected fibers as visualized by electron microscopy. Polarized Raman measurements of the fibers suggested that the nanotubes were highly aligned along the fiber axis, and this alignment was confirmed by high-resolution TEM. The model suggested by these data is that SWNTs wrapped by peptides assemble into fibers through charge−charge interactions of peptides on neighboring nanotubes, a feature that was designed into nano-1. If this model is correct, then it should be possible to modulate the size of the fibers by regulating the ionic strength of the solution, which affects peptide−peptide charge interactions. The addition of NaCl resulted in a dramatic increase in the size of the nano-1/SWNT fibers, from 100 nm in diameter (no salt) to 38 μm (120 mM NaCl). This evidence strongly supports the model that a major determinant of fiber formation is charge−charge interactions of peptides coating the surface of nanotubes. We also found that the amphiphilic additive DMF, which should influence peptide interactions, altered the morphology of the fibers to produce ribbons. Altogether, these data demonstrate that amphiphilic peptides not only solubilize SWNTs, but also can be used to control the assembly of peptide-coated nanotubes into fibers of different sizes and shapes.

A significant advantage of using synthesized peptides to coat nanotubes is that peptide function can be controlled by specifying the amino acid sequence. We exploited this advantage in the present report to engineer a self-assembly function into the peptide, but other capabilities can be envisioned. For example, amphiphilic peptides could be synthesized containing epitopes that bind to specific antibodies. This could lead to the assembly of peptide-wrapped nanotubes onto substrate surfaces coated with patterns of antibodies, a possible step toward arranging carbon nanotubes into architectures useful for electrical circuits and molecular sensing applications.

Acknowledgment. We wish to thank Dr. Bog G. Kim for assistance with SEM measurements and for helpful discussions, and Alfonso Ortiz-Acevedo for general assistance. Financial support for this work was provided by The Robert A. Welch Foundation [AT-1448 (G.R.D.), AT-1326 (I.H.M.)], the Texas Advanced Research Program, [009741-0026-1999 (G.R.D.)], and a University of Texas at Dallas Special Faculty Development Assignment (R.K.D.).

JA029084X

(35) Venkateswaran, U. D.; Rao, A. M.; Richter, E.; Menon, M.; Rinzler, A.; Smalley, R. E.; Eklund, P. C. *Phys. Rev. B* **1999**, *59*, 10 928−10 934.
(36) Rao, A. M.; Chen, J.; Richter, E.; Schlecht, U.; Eklund, P. C.; Haddon, R. C.; Venkateswaran, U. D.; Kwon, Y. K.; Tomanek, D. *Phys. Rev. Lett.* **2001**, *86*, 3895−3898.